Fifth International Conference on CFD in the Process Industries
CSIRO, Melbourne, Australia
13-15 December 2006

A DISTINCT ELEMENT GRANULAR SOLVER/FICTITIOUS DOMAIN METHOD FOR THE NUMERICAL SIMULATION OF PARTICULATE FLOWS

Anthony WACHS and Yannick PEYSSON

Fluid Mechanics Department, Institut Français du Pétrole, 1 & 4, avenue de Bois-Préau, 92852 Rueil-Malmaison, FRANCE

ABSTRACT

In the Oil and Gas industry, many situations are representative of particulate flows : cutting removal in drilling operations, sand management in production, dispersed hydrates transportation in pipeline, ... Particles may be of arbitrary shape and the fluid itself may exhibit non-Newtonian properties. To enhance the comprehension of complex phenomena occurring in moderately or highly concentrated suspensions, we developed a coupled solver based on a Distinct Element Method (DEM) for the granular part and a Finite Element Method for the fluid part. The scale of description is the particle, which implies that our approach may be regarded as a direct numerical simulation. The coupling is achieved by a Distributed Lagrange Multipliers/Fictitious Domain method (DLM/FD) and an operator-splitting algorithm. The DEM enables us to account for actual contacts between particles and consider particles of (polyhedral) arbitrary shape. Simulations up to a few thousands of particles in 2D situations are presented. We illustrate the capabilities of the numerical tool on the sedimentation of particles of polygonal or circular shape in Newtonian and non-Newtonian shear-thinning and thixotropic fluids. Obtained results underline the strong alteration of flow characteristics and the particles pattern.

NOMENCLATURE

p	pressure
$\mathbf{u}$	fluid velocity
ρ_f	fluid density
η	fluid dynamic viscosity
$\mathbf{D}(\mathbf{u})$	strain rate tensor
$\boldsymbol{\lambda}$	distributed Lagrange multiplier to enforce the rigid body motion constraint
ρ_s	particle density
M	particle mass
$\mathbf{I}$	particle moment of inertia
$\mathbf{U}$	particle translational velocity
$\mathbf{X}$	particle position
$\mathbf{w}$	particle rotational velocity
$\mathbf{R}$	particle vector from center to contact point
$\mathbf{F}_{ci}$	collision force on particle i
$\mathbf{g}$	gravitational acceleration
$\mathbf{v}$	variation for the fluid velocity
q	variation for the pressure
$\mathbf{V}$	variation for the particle translational velocity
$\boldsymbol{\xi}$	variation for the particle rotational velocity
α	variation for the Lagrange multiplier
D/Dt	Lagrangian derivative
d/dt	time derivative
$\partial/\partial t$	partial time derivative
k_n	normal contact stiffness
δ_{ij}	overlap between particles i and j
$\mathbf{n}_{ij}$	unit normal vector pointing between the centers of particles i and j
γ_n	normal dynamic friction parameter
γ_t	tangential dynamic friction parameter
k_s	static friction coefficient
μ	Coulomb friction coefficient
m_{ij}	reduced mass of particles i and j
$\mathbf{v}_{rn}$	normal relative velocity between particles i and j
$\mathbf{v}_{tn}$	tangential relative velocity between particles i and j

INTRODUCTION

The comprehension of solid/solid and fluid/solid interactions in highly concentrated particulate flows is of great interest from both fundamental and practical point of views. The hydrodynamics of such complex flows is still poorly understood, even if the fluid phase exhibits simple Newtonian properties. The primary reason for such a poor understanding is the fact that such processes involve phenomena at very different scales from the particle to the flow domain. Therefore, direct numerical simulation at the scale of the particle may be of great help to the understanding of this type of multiphase flows.

In particular, assorted processes of the Oil and Gas industry involve particulate flows at moderate or high concentration (Peysson, 2004). For instance, settling is a key issue for the drilling operation of the well. Drilling muds are designed such that they exhibit specific non-Newtonian properties that prevent the rock cuttings to settle at the bottom hole as the drilling fluid circulation is stopped. In subsea flowlines, the oil is conveyed under low temperature and high pressure that may lead to the formation of hydrates. The use of dispersants can inhibit or limit the aggregation of hydrates into large clusters that can lead to the plugging of the line. However, even in dispersed phase, hydrates may be regarded as solid particles transported in the pipeline by the flowing fluid. Rock cuttings as well as hydrates clusters may be of arbitrary shape and may easily differ from the ideal disk (2D) or sphere (3D) representation.

In this paper, we focus on the sedimentation of particles of isotropic polygonal shape in a Newtonian fluid. The sedimentation of a single particle in a Newtonian or non-Newtonian fluid has been investigated and reviewed by Clift et al. (1978), Chhabra (1993) and McKinley (2002). Deep insights into many aspects of the settling of Newtonian suspensions of spherical particles has been gained by theoretical, experimental and numerical approaches. However, the behaviour of many particles of spherical shape sedimenting in a complex fluid or the one of many particles of polyhedral shape in a Newtonian fluid has been the subject of only a few studies. In particular, let us mention the contribution of Haider and Levenspiel (1989) who investigated the effect of the particle shape on the drag coefficient and terminal velocity of a single non-spherical particle settling in a Newtonian fluid. In the case of spherical particles in

complex fluids, many authors evidenced that settling particles in a viscoelastic (Joseph et al., 1994) or thixotropic shear-thinning (Daugan et al., 2004) fluid aggregate to form columns or chains, in relation to the corridors of low viscosity in the wake of the settling particles.

The dynamic simulation of the particles motion in a fluid is a non-trivial task in relation to the constantly evolving space occupied by the fluid as the particles move. The boundary fitted mesh approach proposed by Hu et al. (2001) and Patankar and Joseph (2001) is very complex in relation to the remeshing requirement of the fluid domain and the corresponding projection of the flow fields on the updated mesh at every time step. In contrast, non-boundary fitted methods, such as the lattice-Boltzmann method (Ladd, 2001) and the Distributed Lagrange Multiplier/Fictitious Domain (DLM/FD) method, are easier to implement and more efficient for the simulation of the motion of a large number of particles. The DLM/FD approach was introduced by Glowinski et al. (1999). The main idea of the method is to fill the region occupied by the particles with the fluid and to treat the particles motion as a constraint of the problem. Then, the particles motion contraint inside the particles boundaries is relaxed thanks to the use of a distributed Lagrange multiplier. This approach was first dedicated to rigid bodies and was applied with success to the simulation of the fluidization of 1024 spheres (3D) and the Rayleigh-Taylor instability of 6400 circular disks (2D) in a Newtonian fluid (Glowinski et al., 1999, 2001). Singh et al.(2000), Yu et al. (2002) and Hwang et al. (2004) extended the method to the case of a viscoelastic fluid whereas Yu et al. (2006) recently considered the case of a shear-thinning and thixotropic fluid as well as a viscoplastic fluid. Yu (2005) even simulated with success the motion of flexible and incompressible bodies in a Newtonian fluid flow.

As the concentration of solid bodies suspended in the fluid exceeds more or less 5%, the probability of collision between particles increases dramatically. As a consequence, this requires the use of proper contact laws and a model (or numerical method) to handle the numerous multi-body collisions. The Distinct Element Method (DEM), also known as Discrete Element Method and introduced by Cundall and Strack (1979), is an attractive approach in which the system is modelled at the particle level. The motion of all particles is computed based on the detection of all collisions and the calculations of the corresponding contact forces. The advantage is the enhanced accuracy of the modelling of the system but it is computationally highly expensive. Recent contributions to the literature using the DEM include Cleary and Prakash (2004) and Wu and Cocks (2006).

In the next section we shortly describe the basic features of the method. Then, we investigate the effect of the particle shape in sedimentation process. We show the significant influence of the particle shape on the drag coefficient and sedimentation time. The last section is devoted to conclusion and perspectives.

MODEL DESCRIPTION

For simplicity, we only consider one particle and a Dirichlet velocity boundary condition on the outer boundary of the flow domain in the description of the formulation below.

Dimensional governing equations

The variational combined momentum equations that govern both the fluid and solid motion has been derived by Glowinski et al. (1999). Here the fluid is assumed to be purely viscous. Therefore the viscosity is either constant for a Newtonian fluid as assumed in this paper or variable for a shear-thinning and thixotropic fluid as considered in our previous paper (Yu et al., 2006). Since the flow is incompressible, the fluid mass conservation reduces to the divergence free constraint of the velocity field i.e. the continuity equation. The governing equations can be non-dimensionalized by introducing the following scales : L_c for the length, U_c for the velocity, L_c/U_c for the time, $\rho_f U_c^2$ for the pressure and $\rho_f U_c^2/L_c$ for the Lagrange multiplier. The complete set of dimensionless governing equations comprise the following two parts :

1. Combined momentum equations

$$\int_\Omega \left(\frac{\partial \boldsymbol{u}}{\partial t} + \boldsymbol{u} \cdot \nabla \boldsymbol{u} \right) \boldsymbol{v} d\boldsymbol{x} - \int_\Omega p \nabla \cdot \boldsymbol{v} d\boldsymbol{x} + \frac{1}{\mathrm{Re}} \int_\Omega 2\boldsymbol{D}(\boldsymbol{u}) : \boldsymbol{D}(\boldsymbol{v}) d\boldsymbol{x} + \int_P \boldsymbol{\lambda} \boldsymbol{v} d\boldsymbol{x} = 0 \tag{1}$$

$$(\rho_r - 1) \left[V_P^* \left(\frac{d\boldsymbol{U}}{dt} - Fr \frac{\boldsymbol{g}}{g} \right) \boldsymbol{V} + \boldsymbol{I}^* \frac{d\boldsymbol{w}}{dt} \boldsymbol{\xi} \right] - \sum_j \boldsymbol{F}_{cj} \boldsymbol{V} - \sum_j \boldsymbol{F}_{cj} \boldsymbol{\xi} \times \boldsymbol{R} - \int_P \boldsymbol{\lambda} (\boldsymbol{V} + \boldsymbol{\xi} \times \boldsymbol{r}) d\boldsymbol{x} = 0 \tag{2}$$

$$\int_P \boldsymbol{\alpha} (\boldsymbol{u} - (\boldsymbol{U} + \boldsymbol{w} \times \boldsymbol{r})) d\boldsymbol{x} = 0 \tag{3}$$

where $V_p^* = M / (\rho_s L_c^3)$ and $\boldsymbol{I}^* = \boldsymbol{I} / (\rho_s L_c^5)$ denote the dimensionless particle volume and moment of inertia, respectively.

2. Continuity equation

$$- \int_\Omega q \nabla \cdot \boldsymbol{u} d\boldsymbol{x} = 0 \tag{4}$$

In the above equations the following dimensionless parameters are introduced :

Reynolds number : $\mathrm{Re} = \dfrac{\rho_f U_c L_c}{\eta}$

Froude number : $Fr = \dfrac{g L_c}{U_c^2}$

density ratio : $\rho_r = \dfrac{\rho_s}{\rho_f}$

Collision model

Binary hard sphere model and soft sphere model are the two categories of collision models for the particulate flows (Crowe et al., 1998). For the hard sphere model, the momentum exchange between two colliding particles takes place exactly at the time when the two particles touch. In contrast, for the soft sphere model, the velocities of colliding particles are determined from the Newton equations of motion with the collision forces of soft potential as a function of the separation or overlap distances between the particles and possibly the particles velocity. A soft sphere model with an artificial repulsive force to prevent any overlap has been proposed by

Glowinski et al. (1999, 2001) and used later by Yu et al. (2002). In our previous paper (Yu et al., 2006), we incorporated a lubrication correction in the collision model.

Here the collisions are described by a soft sphere approach implemented in a DEM granular solver. In this model, the particles are allowed to slightly overlap and the collision forces are calculated based on the overlapping region or distance and the normal and tangential relative velocities at the point of contact (Cundall and Strack, 1979, Cleary and Prakash, 2004, Wu and Cocks, 2006). The considered collision forces comprise:

- the elastic restoring force $\boldsymbol{f}_{el}$:

$$\boldsymbol{f}_{el} = -k_n \delta_{ij} \boldsymbol{n}_{ij} \tag{5}$$

- the viscous dynamic force $\boldsymbol{f}_{dn}$ in the normal direction to account for the dissipative aspect of the contact:

$$\boldsymbol{f}_{dn} = -2\gamma_n m_{ij} \boldsymbol{v}_{rn} \tag{6}$$

where $m_{ij} = \dfrac{M_i M_j}{M_i + M_j}$.

- the tangential friction force $\boldsymbol{f}_t$:

$$\boldsymbol{f}_t = -\min\left\{\mu \left\| \boldsymbol{f}_{el} \right\|, \left\| \boldsymbol{f}_{dt} + \boldsymbol{f}_s \right\|\right\} \boldsymbol{t} \tag{7}$$

where $\boldsymbol{f}_{dt} = -2\gamma_t m_{ij} \boldsymbol{v}_{rt}$ denotes the dissipative frictional contribution and $\boldsymbol{f}_s = -k_t \int_0^{t_c} \boldsymbol{v}_{rt} dt$ the static frictional contribution which behaves like an incremental spring that stores energy during the time of contact t_c. Note that the magnitude of the tangential friction force is limited by the Coulomb frictional limit.

The total collision force acting on a particle i is the sum of the contributions related to the contact with the neighbouring particles j :

$$\boldsymbol{F}_{ci} = \sum_j \boldsymbol{F}_{cij} = \sum_j \left(\boldsymbol{f}_{el} + \boldsymbol{f}_{dn} + \boldsymbol{f}_t \right)_{ij} \tag{8}$$

Computational scheme

Following Glowinski et al. (1999), we employ the first order Marshuk-Yanenko operator splitting algorithm to decouple the system into the following sub-problems :

1. A degenerated Stokes problem : find $\boldsymbol{u}^{n+1/5}$ and $p^{n+1/5}$ such that :

$$\int_\Omega \left(\frac{\boldsymbol{u}^{n+1/5} - \boldsymbol{u}^n}{\Delta t} \right) \boldsymbol{v} d\boldsymbol{x} - \int_\Omega p^{n+1/5} \nabla \cdot \boldsymbol{v} d\boldsymbol{x} = 0 \tag{9}$$

$$-\int_\Omega q \nabla \cdot \boldsymbol{u}^{n+1/5} d\boldsymbol{x} = 0 \tag{10}$$

2. A purely transport problem for inertia : find $\boldsymbol{u}^{n+2/5}$ such that :

$$\int_\Omega \frac{\boldsymbol{u}^{n+2/5} - \boldsymbol{u}^{n+1/5}}{\Delta t} \boldsymbol{v} d\boldsymbol{x} = -\int_\Omega \left(\boldsymbol{u}^{n+1/5} \cdot \nabla \boldsymbol{u}^{n+1/5} \right) \boldsymbol{v} d\boldsymbol{x} \tag{11}$$

3. A viscous problem : find $\boldsymbol{u}^{n+3/5}$ such that :

$$\int_\Omega \frac{\boldsymbol{u}^{n+3/5} - \boldsymbol{u}^{n+2/5}}{\Delta t} \boldsymbol{v} d\boldsymbol{x} + \frac{1}{\mathrm{Re}} \int_\Omega 2\boldsymbol{D}\left(\boldsymbol{u}^{n+3/5}\right) : \boldsymbol{D}(\boldsymbol{v}) d\boldsymbol{x} = 0 \tag{12}$$

4. Update particles velocities ($\boldsymbol{U}^{n+4/5}$, $\boldsymbol{w}^{n+4/5}$) and positions $\boldsymbol{X}^{n+4/5}$

$$\begin{aligned} &\left(\rho_r - 1\right) \left[V_P^* \frac{\boldsymbol{U}^{n+4/5} - \boldsymbol{U}^n}{\Delta t} \boldsymbol{V} + \boldsymbol{I}^* \frac{\boldsymbol{w}^{n+4/5} - \boldsymbol{w}^n}{\Delta t} \boldsymbol{\xi} \right] \\ &- \sum_j \boldsymbol{F}_{cj}{}^n \boldsymbol{V} - \sum_j \boldsymbol{F}_{cj}{}^n \boldsymbol{\xi} \times \boldsymbol{R} = \boldsymbol{0} \\ &\frac{\boldsymbol{X}^{n+4/5} - \boldsymbol{X}^n}{\Delta t} = \boldsymbol{U}^{n+4/5} \end{aligned} \tag{13}$$

5. Fictitious domain problem (fluid/solid interactions) : find $\boldsymbol{u}^{n+1}$, $\boldsymbol{U}^{n+1}$ and $\boldsymbol{w}^{n+1}$ such that :

$$\int_\Omega \frac{\boldsymbol{u}^{n+1} - \boldsymbol{u}^{n+4/5}}{\Delta t} \boldsymbol{v} d\boldsymbol{x} + \int_P \boldsymbol{\lambda} \boldsymbol{v} d\boldsymbol{x} = 0 \tag{14}$$

$$\begin{aligned} &\left(\rho_r - 1\right) \left[V_P^* \frac{\boldsymbol{U}^{n+1} - \boldsymbol{U}^{n+4/5}}{\Delta t} \boldsymbol{V} + \boldsymbol{I}^* \frac{\boldsymbol{w}^{n+1} - \boldsymbol{w}^{n+4/5}}{\Delta t} \boldsymbol{\xi} \right] \\ &- \int_P \boldsymbol{\lambda} \left(\boldsymbol{V} + \boldsymbol{\xi} \times \boldsymbol{r} \right) d\boldsymbol{x} = \left(\rho_r - 1\right) V_P^* Fr \frac{\boldsymbol{g}}{g} \boldsymbol{V} \end{aligned} \tag{15}$$

$$\int_P \boldsymbol{\alpha} \left(\boldsymbol{u}^{n+1} - \left(\boldsymbol{U}^{n+1} + \boldsymbol{w}^{n+1} \times \boldsymbol{r} \right) \right) d\boldsymbol{x} = 0 \tag{16}$$

Computational details

For the sake of consistency, we sum up briefly below the various features of the numerical implementation :

- the spatial discretization scheme for the fluid is a standard Finite Element method with linear triangular element for the pressure and linear triangular element on a twice finer mesh for the velocity (usually called P1/P1ISOP2 interpolation). We also use mass lumping technique for the discretization of the unsteady term such that the corresponding matrix is diagonal.
- the purely transport problem 2 is solved by a wake-like/projection method (Pan and Glowinski, 2000), avoiding the use of any upwinding technique.
- saddle-point problems 1 and 5 are solved by an efficient preconditioned Uzawa/conjugate gradient algorithm.
- in problem 4, the integration of the equations of motion is actually carried out by an explicit leap-frog scheme (Cundall and Strack, 1979, Wu and Cocks, 2006). Since the time scale of the contact between two particles is much smaller than the fluid time scale, the time interval Δt in problem 4 is sub-divided in N time intervals. In other words, we solve N times problem 4 with a time step $\Delta t/N$ for every fluid time step Δt.
- in problem 4, most of the computation time is dedicated to the search of the connection between particles and the calculation of the overlapping regions. To reduce at most this task, we use an efficient linked cell algorithm based on an underlying mesh for the location of the particles.
- in problem 5, the spatial discretization of the Lagrange multiplier for the rigid body motion constraint is based on the collocation point method proposed by Glowinski et al. (1999, 2001). It was found that a minimim of 8 elements on the particle diameter is necessary for an acceptable accuracy of the solution.

RESULTS

We focus here on the sedimentation of 2D isotropic polygonal particles in a Newtonian fluid (previous papers (Yu et al., 2006, Yu and Wachs, 2006) were dedicated to the sedimentation in a non-Newtonian fluid). To account for the shape of the particle, we follow Haider and Levenspiel (1989)'s 3D sphericity concept and introduce a similar concept of circularity in 2D, Φ, defined as:

$$\Phi = S_p / S_d \tag{21}$$

where S_p and S_d are the surfaces of the polygon and the disk, respectively. In (21), polygon and disk perimeters are identical. In the case of an isotropic polygonal particle, Φ reads :

$$\Phi = \frac{\pi}{n_p}\cot an\left(\frac{\pi}{n_p}\right) \tag{22}$$

where n_p is the number of sides of the polygon.

Sedimentation of a single particle in an infinite domain

Here we study the influence of the particle shape on the drag coefficient of a single particle settling in an infinite domain as a function of the Reynolds number. The chosen characteristic length and velocity are the particle projected length L_p and the terminal settling velocity U_∞, respectively. The density ratio ρ_r is set to 1.1. The infinite domain is modelled by considering a rectangular flow domain that expands as far as 200 times the particle diameter in both directions.
The drag coefficient C_d is computed as :

$$C_d = \frac{(\rho_s - \rho_f)gL_p}{0.5\rho_f U_\infty^2} \tag{23}$$

Table 1 gathers the various shapes considered and their corresponding circularity.

Particle shape	Circularity Φ
Disk	1
Decagon	0.967
Hexagon	0.907
Square	0.785
Triangle	0.605

Table 1. Particles shape and circularity

In the range of Reynolds numbers [1,35] considered, the velocity profile is stable as the particle reaches the terminal velocity. Indeed, the Von Karmann vortex shedding regime is well known to start above Re=50-70.
The mesh together with the DLM/FD set of points are illustrated in figure 1. It comprises 29768 triangular elements for the pressure (15129 pressure unknowns) and 119072 for the velocity (179586 velocity unknowns). In the single particle case, the particle is accurately described with 40 elements on the particle diameter, as shown in figure 1(b). Results obtained with coarser meshes (20 and 12 elements on the particle diameter) give comparable results. Numerical experiments revealed that the lowest bound for an acceptable accuracy seems to be 8 elements on the particle diameter. The time step is set to $\Delta t=10^{-3}$. At the initial time, the fluid and solid velocity are zero. The simulation is run until the particle reaches its terminal settling velocity. The average number of time steps required to reach the steady state is 50000 for a total computation time of more or less 24hours on a 3.0GHz Linux sequential workstation.

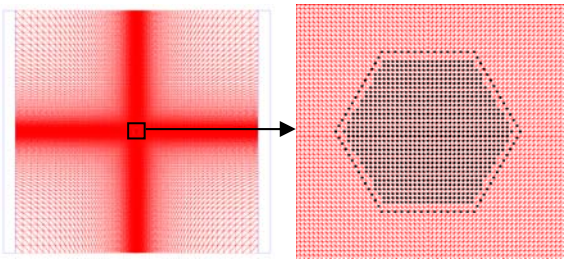

(a) Flow domain (b) Zoom on the particle

Fig 1. Mesh and DLM/FD set of points in the case of a single particle (hexagon) settling in an infinite domain

Figure 2 presents the evolution of the drag coefficient as a function of the Reynolds number for the different polygonal particles. For all shapes, the drag coefficient decreases when the Reynolds number increases. This trend has been reported by many studies in the case of the flow past a fixed circular cylinder (for instance see Lima e silva et al. (2003)).

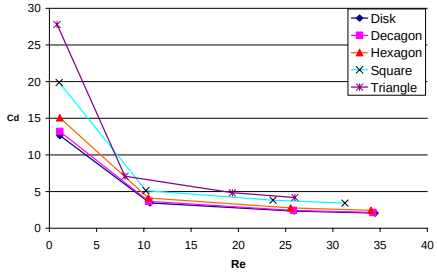

Fig 2. Evolution of the drag coefficient as a function of the Reynolds number for the various shapes considered

In figure 3, we compare our computed drag coefficients for a disk with the results of Lima e silva et al. in the range [10,50] (to be consistent with the drag coefficient formula of Lima e silva et al., we plot in figure 3 : C_d^*=Cd.π/4). The agreement is very satisfactory. We evidence here that our non boundary-fitted numerical method dedicated to the free motion of solid bodies in a fluid is able to provide accurate results in the case of a disk and extends the results to particles of polygonal shape.

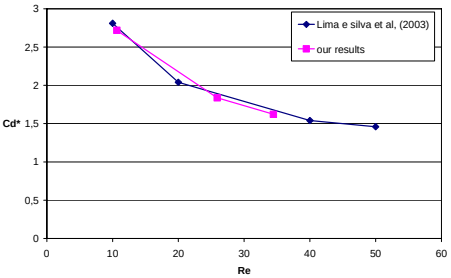

Fig 3. Evolution of the drag coefficient C_d^*=Cd.π/4 as a function of the Reynolds number for a disk : comparison with the numerical results of Lima e silva et al. (2003)

Figure 4 shows the influence of the circularity on the drag coefficient in the range of Reynolds numbers [1,35]. For a given Reynolds number, the ratio of the drag coefficients between a triangle and the ideal disk is of the order of 2. This sheds light on the importance of the particle shape on the sedimentation process, especially in terms of terminal settling velocity and sedimentation time.

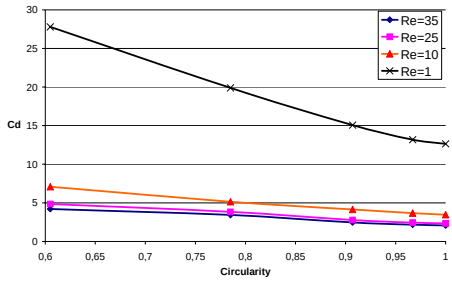

Fig 4. Evolution of the drag coefficient as a function of the circularity for different Reynolds numbers (values of Reynolds number correspond to the disk case)

Sedimentation of 300 particles in a closed box : effect of the shape

In this subsection we investigate the effect of the particle shape on the sedimentation of 300 particles in a closed box. The study is restricted to the two following extreme cases : the ideal disk and the isotropic triangle. The chosen characteristic length and velocity are the disk diameter d and the terminal settling velocity U_∞ of a single disk in an infinite domain, respectively. The density ratio ρ_r is set to 1.1. The Reynolds and Froude numbers based on U_∞ are 25 and 12.5, respectively.

The flow domain is a rectangular closed box the dimensions of which are $W \times H = 20d \times 60d$. A zero velocity (no slip) Dirichlet condition is imposed on all boundaries. At the initial time, the particles are drifted at the top of the box in a random fashion and the fluid and particles velocity is zero. The simulation is run until all particles have settled to the bottom of the box.

The mesh is a structured and constant grid size mesh. It comprises 120 and 360 points in the width and height direction, respectively. This means 153600 triangular elements for the pressure (77441 pressure unknowns) and 614400 for the velocity (616962 velocity unknowns).

The time step is set to $\Delta t=5.10^{-3}$. In both cases (disks and triangles), 50000 time steps are computed for a total computation time of 8 days on a 3.0GHz Linux sequential workstation.

Figure 5 presents snapshots of the particles pattern and vertical velocity contours. The first stages of the sedimentation process highlights a hydrodynamic Rayleigh-Taylor (RT) instability (t=31.25) involving the pack of particles which later breaks into small clusters or individual particles (t=62.5). Finally, the particles settle at the bottom of the box and the fluid returns to rest.

Figure 6 plots the time evolution of the mean vertical velocity and position (rescaled between 0 and 1) of the particles. The RT hydrodynamic instability is triggered later in the case of the disks (first velocity peak) but once the pack of particles breaks into many small clusters or individual particles, disks settle around 10% faster than triangles. The actual Reynolds number based on the mean settling velocity is around 4. The drag coefficient of a triangle settling in an infinite domain is twice larger than the one of a disk. This may partly explain the faster sedimentation process of disks but other more complex phenomena related to the solid/solid and fluid/solid interactions that require a deeper analysis, as the particles pattern for instance, may be responsible as well.

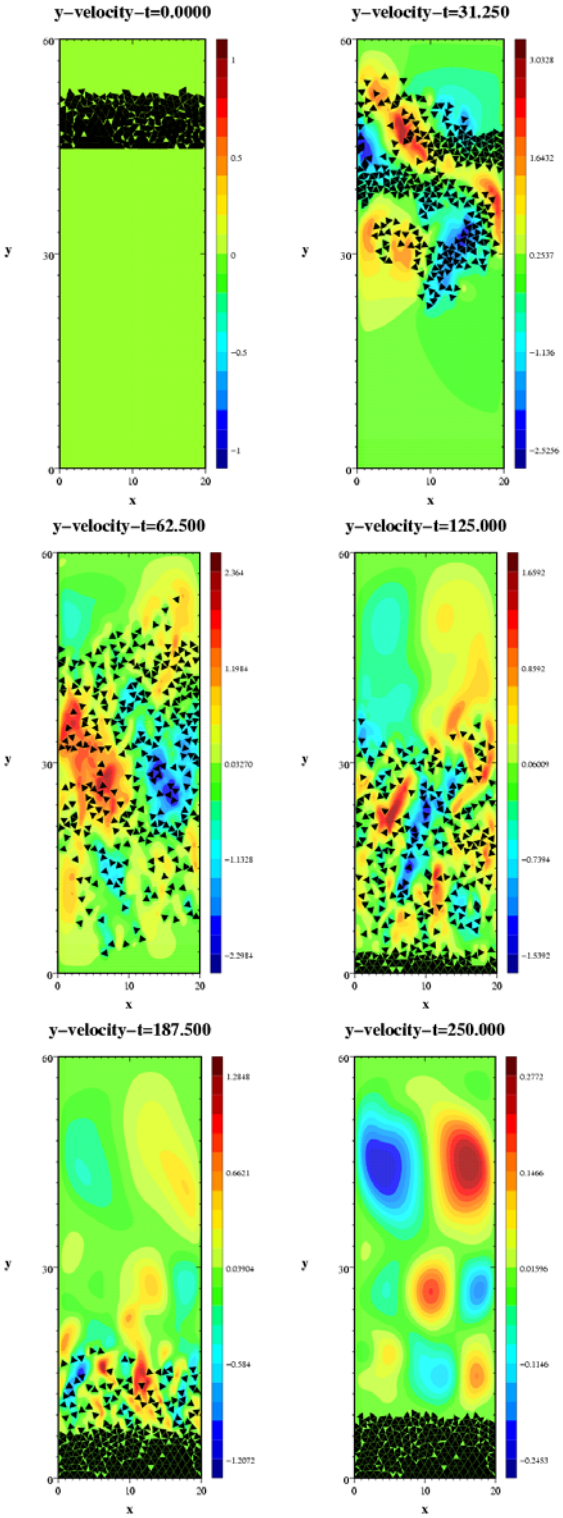

Fig 5. Sedimentation of 300 triangles in a closed box : particles pattern and contours of vertical velocity

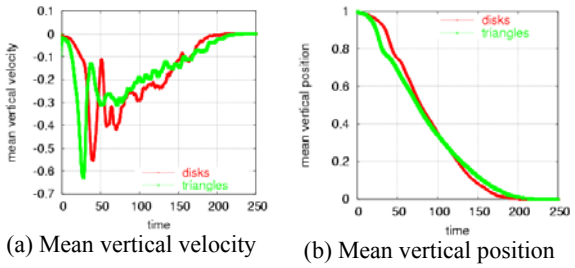

(a) Mean vertical velocity (b) Mean vertical position

Fig 6. Comparison between disks and triangles in the case of the sedimentation of 300 particles in a closed box

Sedimentation of 2500 disks in a closed box

We illustrate here the capabilities of the numerical code to simulate particulate flows with a few thousands of particles.

Figure 7 presents a snapshot of a sedimentation of 2500 disks in which the initial state is an homogeneous lay out of the particles (solid concentration is 40%). Here the disks are twice smaller than in the previous section. This requires the definition of a finer mesh and the corresponding computation time for the complete sedimentation in around 30 days.

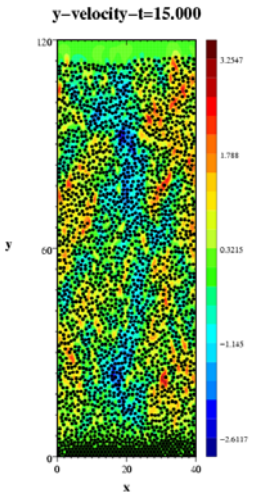

Fig 7. 2500 disks settling in a closed box

CONCLUSION

We presented a novel method to tackle the numerical simulation of particulate flows at moderate or high concentration. To the best of our knowledge, it is the first time the coupling of a DEM solver with a Finite Element DLM/FD method is reported in the literature. The resulting tool enables us to consider particles of arbitrary (polyhedral) shape in a Newtonian or non-Newtonian fluid. Here we applied our method to the effect of the particle shape in a 2D sedimentation process in a Newtonian fluid. Obtained results underline the increase of the drag coefficient with decreasing circularity in the case of a single particle settling in an infinite domain at Reynolds number in the range [1,35]. Finally, the sedimentation of a large number of particles in a closed box at Re=4 exhibits complex particles patterns and confirms that particles of low circularity (triangles) settle slower than disks. At the practical level, the consideration of a large number of particles (tens of thousands) is limited by the computation time on a sequential workstation. To overcome this difficulty, our next objective is to upgrade to a full parallel version of the code.

REFERENCES

CHHABRA, R.P., (1993), "Bubbles, Drops and Particles in Non-Newtonian Fluids", CRC Press, Boca Raton, FL.

CLEARY, P.W. and PRAKASH, M., (2004), "Discrete-element modelling and smoothed particle hydrodynamics: potential in the environmental sciences", Phil. Trans. R. Soc. Lond. A, 362, 2003–2030.

CLIFT, R., GRACE, J. and WEBER, M.E.,(1978), "Bubbles, Drops and Particles", Academic Press, New York.

CROWE, C., SOMMERFELD, M. and TSUJI, Y., (1998), "Multiphase flows with droplets and particles", CRC press.

CUNDALL, P.A. and STRACK, O.D.L., (1979), "A discrete numerical model for granular assemblies", Geotechnique, 29, 47-65.

DAUGAN, S., TALINI, L., HERZHAFT, B., ALLAIN, C. and PEYSSON, Y., (2004), "Sedimentation of suspensions in shear-thinning fluids", Oil Gas Sci. Techno.: Rev. IFP, 59, 71-80.

GLOWINSKI, R., PAN, T.W., HESLA, T.I. and JOSEPH, D.D., (1999), "A distributed Lagrange multiplier/fictitious domain method for particulate flows", Int. J. of Multiphase Flow, 25, 755-794.

GLOWINSKI, R., PAN, T.W., HESLA, T.I., JOSEPH, D.D. and PERIAUX, J. (2001), "A fictitious domain approach to the direct numerical simulation of incompressible viscous flow past moving rigid bodies: application to particulate flow", J. of Comput. Phys., 169, 363-426.

HAIDER, A. and LEVENSPIEL, O., (1989), "Drag coefficient and terminal velocity of spherical and non-spherical particles", Powder Technology, 58, 63-70.

HU, H.H., PATANKAR, A. and ZHU, M.Y., (2001), "Direct numerical simulations of fluid-solid systems using the arbitrary Lagrangian-Eulerian technique", J. Comput. Phys., 169, 427-462.

HWANG, W.R., HULSEN, M.A. and MEIJER, H.E.H., (2004), "Direct simulations of particle suspensions in a viscoelastic fluid in sliding bi-periodic frames", J. of Non Newtonian Fluid Mech.., 121, 15-33.

JOSEPH, D.D., LIU, Y., POLETTO, M. and FENG, J., (1994), "Aggregation and dispersion of spheres falling in viscoelastic liquids", J. of Non Newtonian Fluid Mech., 54, 45-86.

LADD, A.J.C. and VERBERG, R., (2001), "Lattice-Boltzmann simulations of particle-fluid suspensions", J. Stat. Phys., 104, 427-462.

LIMA E SILVA, A.L.F., SILVEIRO-NETO, A. and DAMASCENO, J.J.R., (2003), "Numerical simulation of two-dimensional flows over a circular cylinder using the immersed boundary method", J. Comput. Phys., 189, 351-370.

McKINLEY, G., (2002), "Transport Processes in Bubbles, Drops and Particles", 2nd ed., Taylor & Francis, New York.

PATANKAR, N.A. and JOSEPH, D.D., (2001), "Modeling and numerical simulation of particulate flows by the Eulerian-Lagrangian approach", Int. J. of Multiphase Flow, 27, 1659-1684.

PAN, T. W. and GLOWINSKI, R., (2000), "A projection/wave like equation method for the numerical simulation of incompressible viscous fluid flow modeled by the Navier&Stokes equations", Comp. Fluid. Dyn. Journal, 9/2, 28-42.

PEYSSON, Y., (2004), "Solid/Liquid dispersion in Drilling and Production", Oil Gas Sci. Techno.: Rev. IFP, 59, 11-21.

SINGH., P., JOSEPH, D.D., HESLA, T.I., GLOWINSKI, R. and PAN, T.W., (2000), "A distributed Lagrange multiplier/fictitious domain method for viscoelastic particulate flows", J. of Non Newtonian Fluid Mech.., 91, 165-188.

YU, Z., PHAN-THIEN, N., FAN, Y. and TANNER, R.I., (2002), "Viscoelastic mobility problem of a system of particles", J. of Non Newtonian Fluid Mech.., 104, 87-124.

YU, Z., WACHS, A. and PEYSSON, Y., (2006), "Numerical simulation of particle sedimentation in shear-thinning fluids with a fictitious domain method", J. of Non Newtonian Fluid Mech.., 136, 126-139.

YU, Z. and WACHS, A., (2006), "A fictitious domain method for dynamic simulation of particle sedimentation in Bingham fluids", submitted to J. of Non Newtonian Fluid Mech..

YU, Z., (2005), "A DLM/FD method for fluid/flexible body interaction", J. of Comput. Phys., 207, 1-27.

WU, C.Y. and COCKS, A.C.F, (2006), "Numerical and experimental investigations of the flow of powder into a confined space", Mech. of Materials, 38, 304-324.